

# Flow regimes and structure in pool and weir fishways<sup>1</sup>

S.A. Ead, C. Katopodis, G.J. Sikora, and N. Rajaratnam

**Abstract:** The main objective of this work was to study the hydraulics of pool and weir fishways, for wider range of bed slopes, weir spacing, and heights, so that they can be designed to allow the passage of different species and sizes of fish. This laboratory study contains the results of 435 experiments, including the flow regimes, main flow characteristics and velocity profiles for several discharges. The flow regimes may be classified into plunging, transitional, streaming, and supercritical jet flows. A diagram has been developed to predict the different flow regimes using two dimensionless variables,  $Q_{1*}$  and  $L/p$ . The dimensionless discharge  $Q_{1*}$  for plunging flows was found to follow the Rehbock equation while  $Q_{2*}$  assumed a constant value equal to 5.75 for streaming flows. Velocity profiles in plunging as well as in streaming flows were found to be similar and correlations have been developed for the velocity and length scales. If the present work is considered to be a scale-model study, the scale would be approximately 10.

**Key words:** fishways, pools and weirs, hydraulics, turbulent flow, energy dissipation, fisheries management.

**Résumé :** L'objectif principal de ce travail était d'étudier l'aspect hydraulique des fosses et des gradins des passes migratoires afin de déterminer une grande plage de pentes du fond, d'espacement et de hauteurs des gradins, dans le but d'obtenir une conception adéquate pour passer plusieurs espèces différentes de poissons de dimensions différentes. Cette étude de laboratoire contient les résultats de 435 expériences, incluant les régimes d'écoulement, les caractéristiques de l'écoulement principal et les profils de vitesse pour différentes décharges. Les régimes d'écoulement peuvent être classés en écoulements déferlants, transitoires, noyés et supercritiques. Un diagramme a été développé pour prédire les différents régimes d'écoulement en utilisant deux variables sans dimension,  $Q_{1*}$  et  $L/p$ . Il a été découvert que la décharge sans dimension  $Q_{1*}$  pour les écoulements déferlants suit l'équation de Rehbock alors que  $Q_{2*}$  prend une valeur constante égale à 5,75 pour les écoulements noyés. Les profils de vitesse pour les écoulements déferlants et noyés se sont avérés similaires et des corrélations ont été développées pour les échelles de vitesse et de longueur. Si le travail actuel est considéré comme une étude d'un modèle-échelle, l'échelle serait approximativement de 10.

**Mots clés :** passes migratoires, fosses et gradins, hydraulique, débit turbulent, dissipation d'énergie, gestion de la pêche.

## Introduction

Pool and weir fishways are one of the main types of fishways that are generally used for upstream passage of fish past obstructions in streams and rivers (Katopodis 1999). A pool and weir fishway consists of a number of pools produced by a series of weirs (see Fig. 1a). Water flows downstream over these weirs from one pool to the next downstream. Fish pass over these weirs, after resting in the pools, by swimming over them

using their burst speed or by jumping over them, like salmon and trout. Pool and weir fishways are built, sometimes with the addition of orifices on the weir walls (see Fig. 1b). These fishways, with or without orifices, are generally designed for a head drop per pool of approximately 0.30 m for anadromous salmon (Clay 1961). The slope of these fishways varies from 1 on 8 to 1 on 10.

Adapting fishways for a variety of species, especially non-salmonids is of growing interest in Canada, the USA, and many other countries. Although thousands of fishways have been constructed around the world, few fishways exist that specifically target species larger or smaller than adult salmon (Katopodis 1999). For example, lake sturgeon (*Acipenser fulvescens*) is a primary species of concern in the Canadian Provinces of Ontario, Manitoba, and Saskatchewan, as well as the Midwest States of Wisconsin and Michigan in the USA, and Hokkaido, in Japan. Passage of juvenile salmon and juveniles of other species is also of increased concern. Space requirements and suitable hydraulic conditions in the plunging and streaming flow regimes (Figs. 1c–1d) for passage of large and small fish of various species necessitated a more comprehensive study of pool and weir fishways over a wide range of floor slopes  $S_0$ , weir spacing  $L$ , and weir heights  $p$  (Katopodis 1995a, 1995b). Specific objectives for this study were: to obtain more extensive

Received 10 July 2003. Revision accepted 16 October 2003. Published on the NRC Research Press Web site at <http://jces.nrc.ca/> on 19 August 2004.

**S.A. Ead.** Department of Civil Engineering, Ain Shames University, Cairo, Egypt.

**C. Katopodis.** Regional Habitat Engineer, Fisheries and Oceans Canada, Winnipeg, MB, Canada.

**G.J. Sikora.** City of Red Deer, Red Deer, AB, Canada.

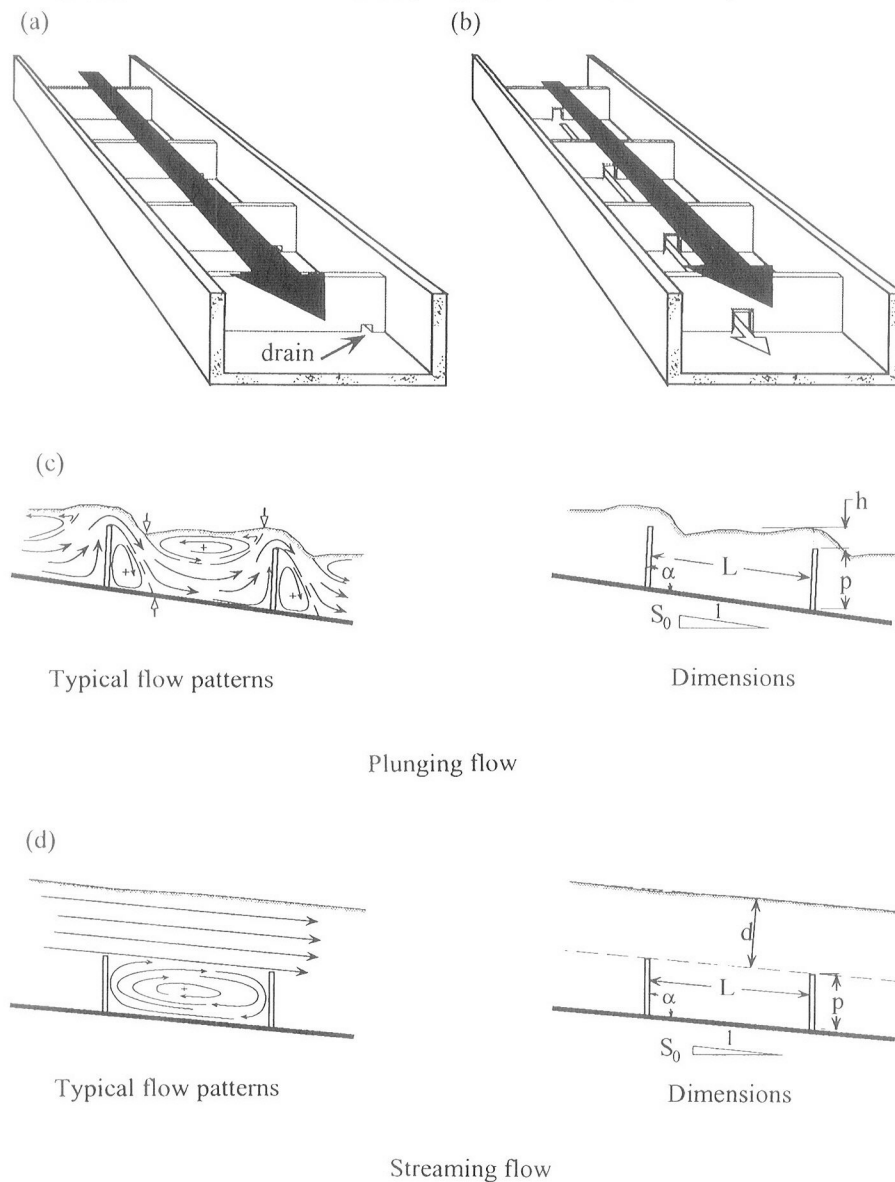
**N. Rajaratnam.**<sup>2</sup> Department of Civil and Environmental Engineering, University of Alberta, Edmonton, AB, Canada.

Written discussion of this article is welcomed and will be received by the Editor until 31 January 2005.

<sup>1</sup>This article is one of a selection of papers published in this Special Issue on Environmental Hydraulics.

<sup>2</sup>Corresponding author (e-mail: [Nrajaratnam@ualberta.ca](mailto:Nrajaratnam@ualberta.ca)).

Fig. 1. (a) Pool-weir fishway, (b) pool-weir-orifice fishway, (c) plunging flow, and (d) streaming flow.



data on plunging and streaming flows, to extend the range of floor slope to 30%, to study the effect of spacing and height of weirs on the flow regimes, and to study the velocity field and energy dissipation in the pools for plunging and streaming flows. Based on the results of this study, some of the earlier equations for pool and weir fishways have been modified and extended. The results of this laboratory investigation are believed to be of general interest and hence are presented in this paper.

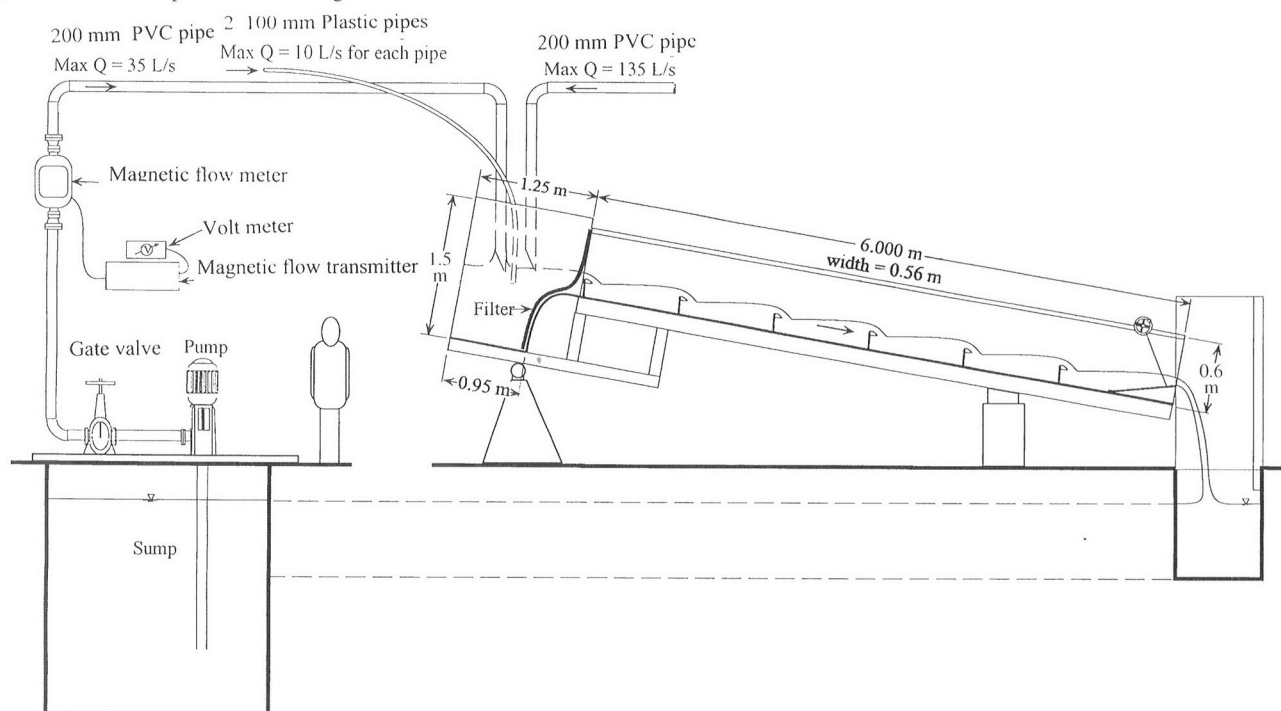
### Experimental arrangement and experiments

Experiments on the pool and weir fishway were performed in a rectangular flume, 6 m long, 0.56 m wide, and 0.60 m deep with an adjustable slope (see Fig. 2) with plexiglas side

walls and an aluminum bed. This flume with a head-tank was supported on two pivots and by simply adjusting the downstream end of the flume, the slope of the model fishway could be changed. Plexiglas weirs with a thickness of about 10 mm were fastened and sealed to the side walls with sheet metal brackets and bolted at an angle that would result in a vertical weir for a 10% bed slope. Water for the fishway was pumped from the laboratory sump into the head tank. A total of four pumps were used to supply the required discharge up to a maximum of 165 l/s and the discharge was measured with magnetic flow meters located in the supply lines.

A total of 435 experiments were performed, and complete details are provided in Sikora (1997). To identify individual experiments, a coding system (for example, 1WB10-065 in Fig. 4*l*)

Fig. 2. Sketch of experimental arrangement.



was used that identifies the weir height, fishway type, weir spacing, bed slope (%) and discharge  $Q$  in litres per second. Starting from the left and proceeding to the right, the first number corresponds to the weir height  $p$ , and will be either 1, 3/4, or 1/2. These numbers indicate that the weirs for each respective arrangement were typically full, three quarters, or one half the normally used value which was 141 mm (in the model). The second letter W indicates that experiments were conducted on weirs only and no orifices or chutes were incorporated into the design. The next letter (A, B, C, and D) defines the weir spacing used, with  $L$  equal to 685, 335, 166, and 77 mm for the A, B, C, and D series respectively. The next two numbers define the slope of the bed in percent. The final three numbers represent the discharge in litres per second. In the example listed above, the experiment IWA05-010 describes the arrangement as a full weir height pool and weir fishway with a A class weir spacing, 5% bed slope, and a discharge of 10 L/s.

For the weirs with a height of  $p = 141$  mm (in the model), a total of 240 experiments were performed with four spacings (A–D), five slopes (5 to 30%) and 12 discharges (5 to 165 L/s). A similar but shorter series of experiments were performed for weirs with 3/4 and 1/2 the full weir height of 141 mm. If the fishways in this study are treated as scale models, the scale will be approximately 10. The weir height of 141 mm and spacing of 335 mm (B class) are close to the commonly used values. For both 3/4 and 1/2 weir height groups of experiments ( $p = 119$  mm, and 74 mm), the closely packed D class weir spacing was omitted since plunging flow occurred only for extremely small discharges.

A total of 435 water surface profiles were measured in order to provide insight into what type of flow regime was present for each and every geometrical configuration and discharge. These measurements were also used to determine the head  $h$  over the weirs for plunging flows and the streaming depth  $d$  for streaming flows, which were used to calculate the dimensionless discharge parameters  $Q_+$  and  $Q_*$  proposed by Rajaratnam et al. (1988). Water surface profiles were measured in the middle of the fishway with a point gauge capable of measuring to 0.3 mm, covering one pool and two half pools on either side. Typical water surface profiles are shown in Figs. 3a–3d (and all the profiles are available in Sikora 1997).

In addition to the water surface profile measurements, a photographic record was also made of all the experiments (which is available in Sikora et al. 1996). The velocity field in the centerplane of the fishway was measured for several flows, with a pitch probe (Rajaratnam and Muralidhar 1967) of 9.3 mm height. Figures 4a–4c show the velocity field, in plunging flows, for experiments IWA10-035, 3/4 WA10-035, and 1/2 WA10-035 whereas Fig. 4d shows the velocity field, in a streaming flow, for experiment IWB10-065. Figures 4a–4d also show the locus of the maximum velocity as well as the lines delineating the surface and the confined eddies.

## Analysis of experimental results

### Plunging, streaming, and other regimes

Clay (1961) was one of the first researchers to describe the plunging, transitional, and streaming or shooting flow regimes

Fig. 3. Water surface profiles for several experiments.

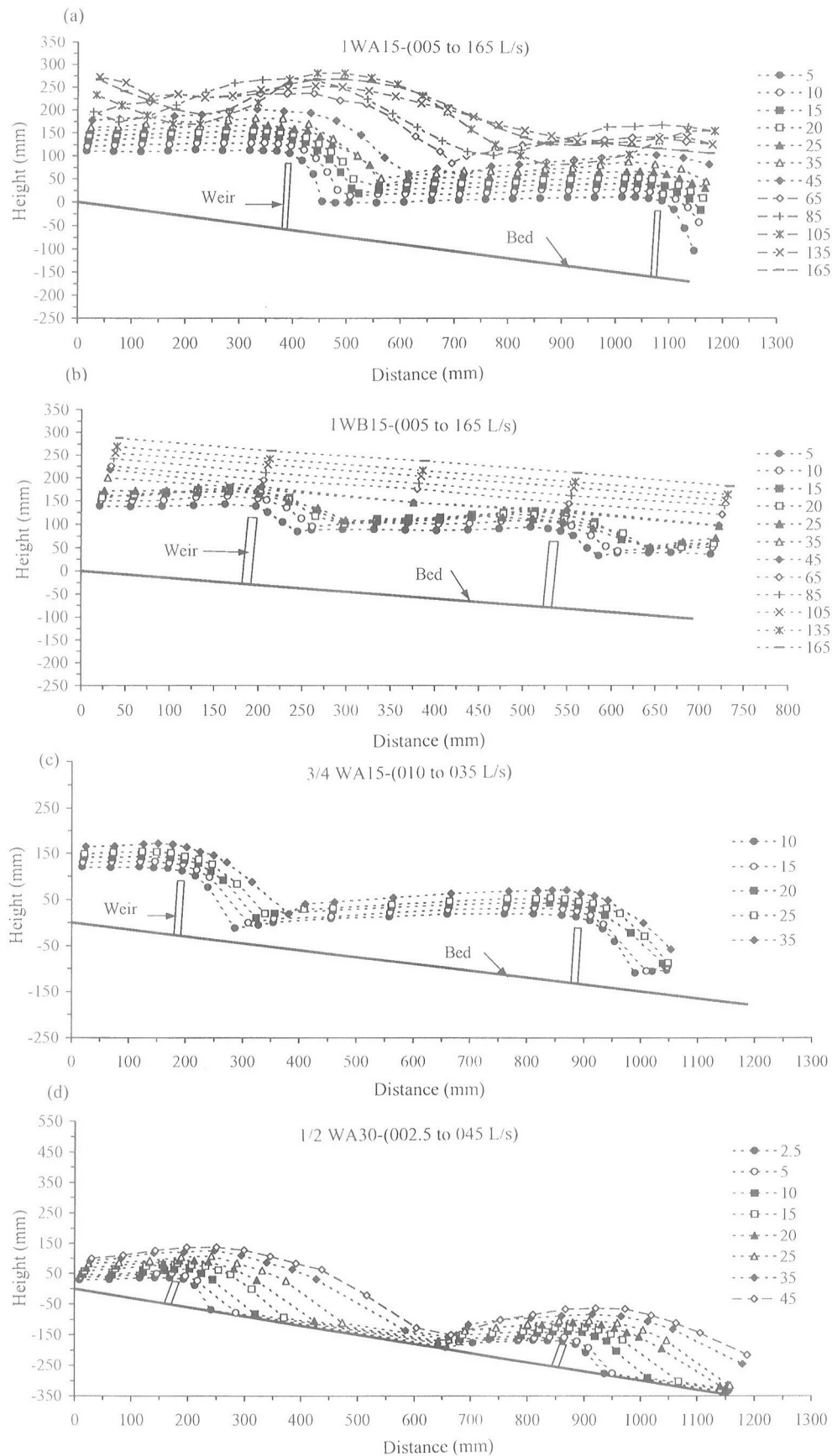
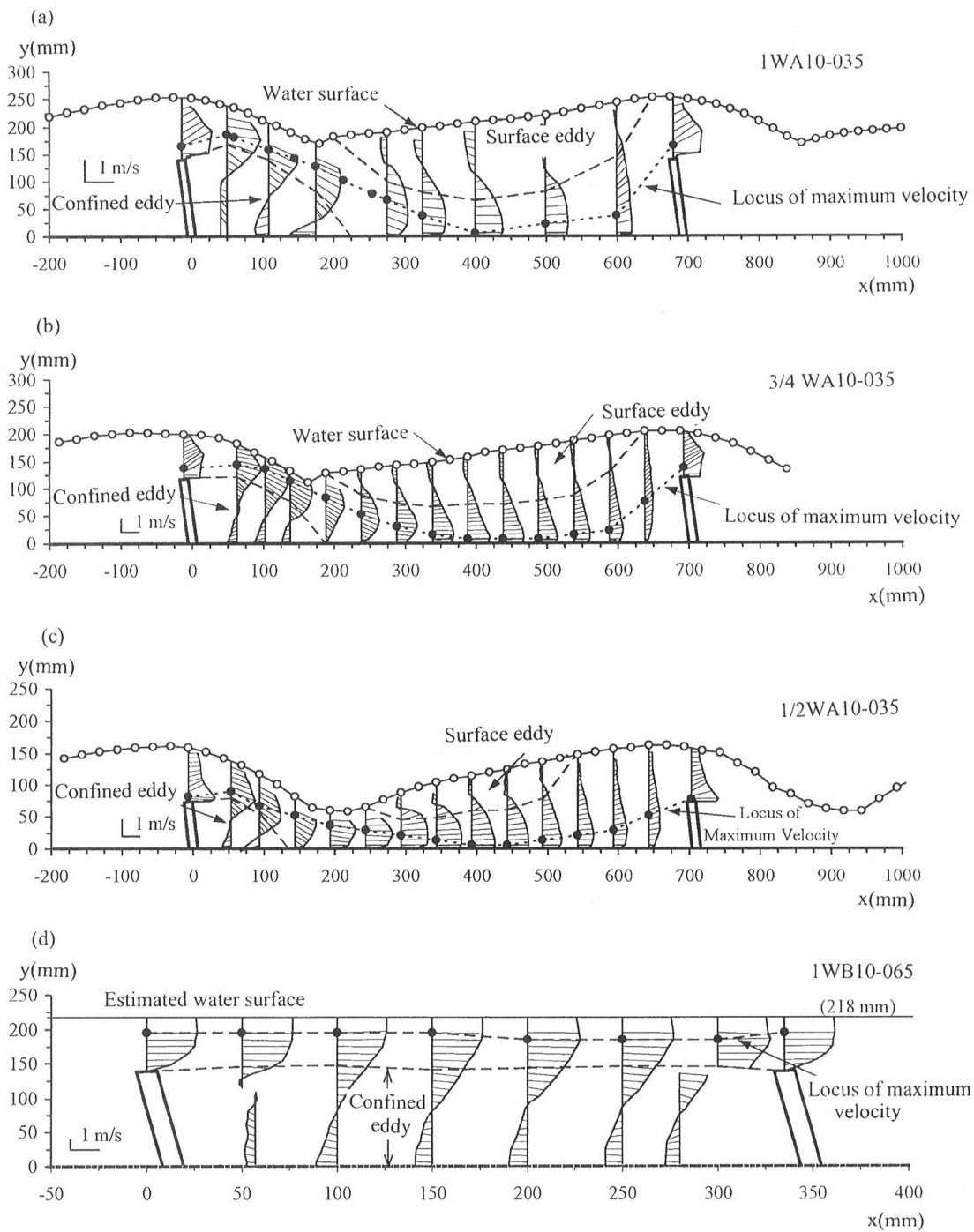


**Fig. 4.** Velocity profiles in the pools for (a-c) plunging and (d) streaming flows.



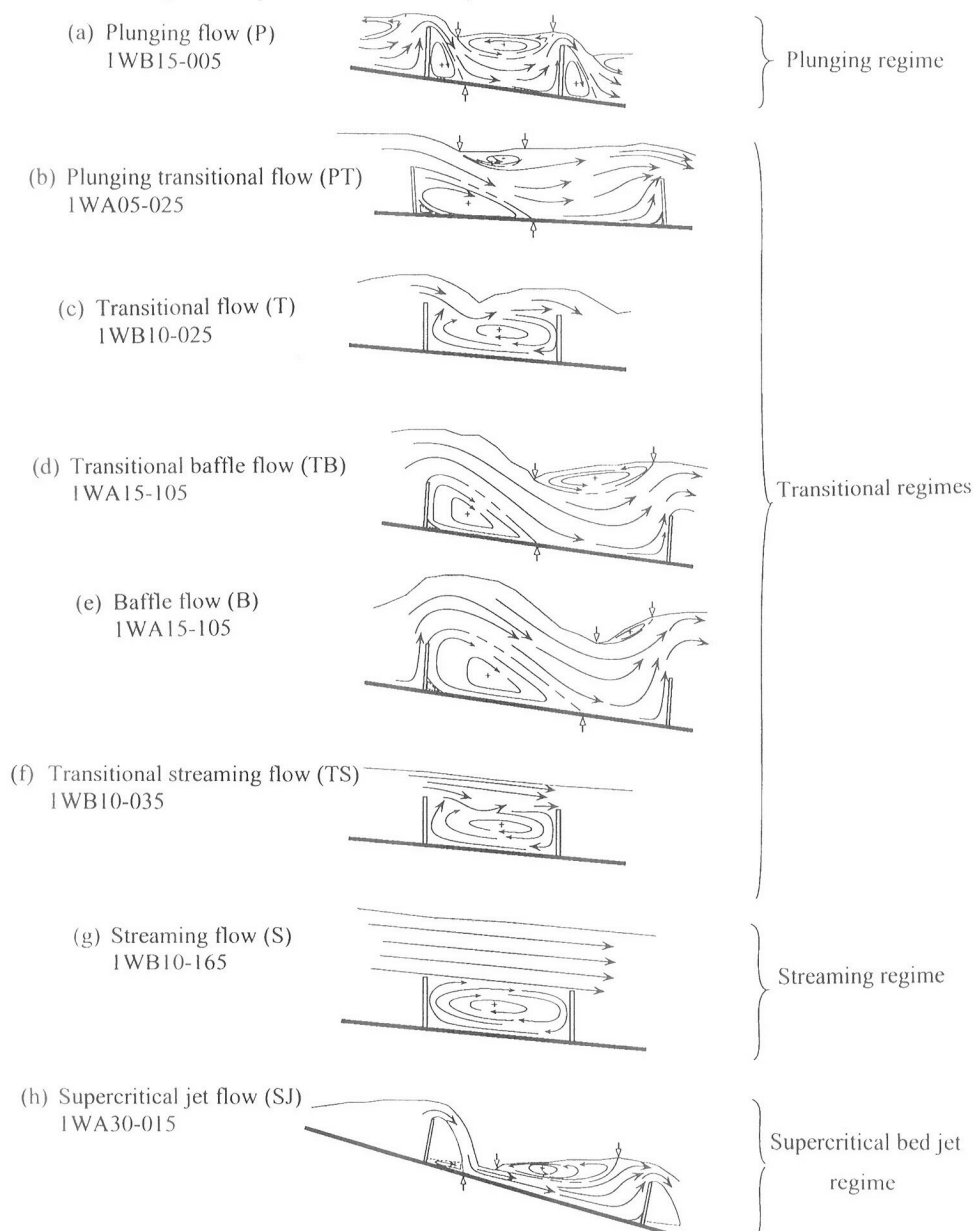
in pool and weir fishways. Rajaratnam et al. (1988) confirmed the observations of Clay and developed quantitative descriptions for these regimes. In the plunging flow regime, they found that the dimensionless discharge  $Q_+$  is approximately equal to 0.61, where  $Q_+$  is defined as

$$[1] \quad Q_+ = \frac{Q}{b_0 \sqrt{g} h^{3/2}} = \frac{2\sqrt{2}}{3} C_d$$

where  $Q$  is the discharge,  $b_0$  is the fishway width,  $g$  the acceleration due to gravity, and  $h$  is the head over the weirs (measured at the location where it has the maximum value). In the streaming (or skimming) flow regime, Rajaratnam et al. (1988) found that the dimensionless discharge  $Q_*$  defined by the equation

$$[2] \quad Q_* = \frac{Q}{b_0 d^{3/2} \sqrt{g S_0}} = \sqrt{\frac{2}{C_f}}$$

Fig. 5. Detailed sketches of flow regimes in pool and weir fishways.



is approximately equal to  $1.5(L/d)^{0.5}$  where  $d$  is the streaming flow depth,  $S_0$  is the fishway slope,  $C_f$  the coefficient of fluid friction, and  $L$  is the length of pool. They also found that the transition from the plunging to the skimming flow occurred when the parameter  $Q_{1*}$  defined as

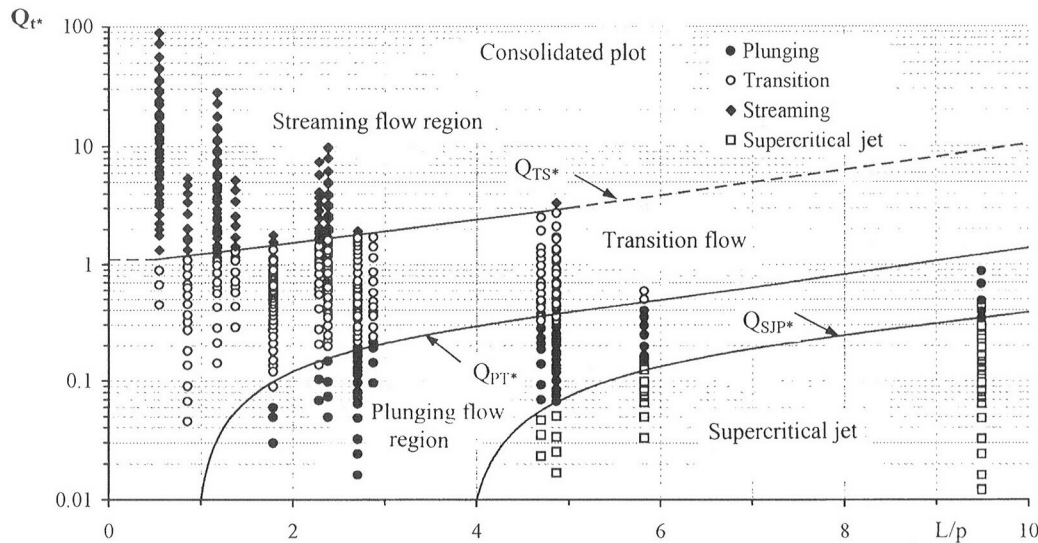
$$[3] \quad Q_{1*} = \frac{Q}{\sqrt{g b_0 S_0 L^3 / 2}}$$

was approximately equal to 0.25.

These regimes are indeed the major flow regimes found in traditional pool and weir fishways. However, it was found in this study that when the bed slope, weir spacing, and height are varied over a larger range, several sub-regimes were found to exist in addition to a supercritical jet flow (as indicated in

Fig. 5a-5h). Figure 5a shows a plunging flow where a plunging jet dives into the pool creating two rotating cells or eddies. The first eddy with a clockwise rotation, is located under the plunging jet from the weir and is also bounded by the bed and the weir. The second eddy is positioned near the surface and forms immediately downstream of the line where the plunging jet enters the pool. This counterclockwise rotating surface eddy is somewhat similar to the surface roller of a hydraulic jump. Both these eddies were typically uniform across the width of the flume and varied in length depending on the physical dimensions of the pool, the discharge, and the slope. Other subtle and less obvious flow characteristics are the three lines indicated by the hollow arrows in Fig. 5a. The first line is where the plunging jet impinges on the bed of the flume. The other two

Fig. 6. Consolidated plot of the flow regimes in pool and weir fishways.



lines represent the beginning and the end of the surface eddy. Observing the location of these lines relative to the length of the pool  $L$ , indicates the changes in the flow patterns as the flow parameters change.

Figure 5b shows a typical flow pattern and water surface profile for plunging-transitional flows (PT). Although this flow pattern shares some resemblance to the plunging regime, there are significant differences in the flow structure and the water surface profiles. The surface roller is relatively shorter and shallower. The confined roller, located under the nappe, expands downstream to the middle of the pool. After closer observations, it was evident that this plunging-transitional regime occurs at, or shortly after weir submergence sets in.

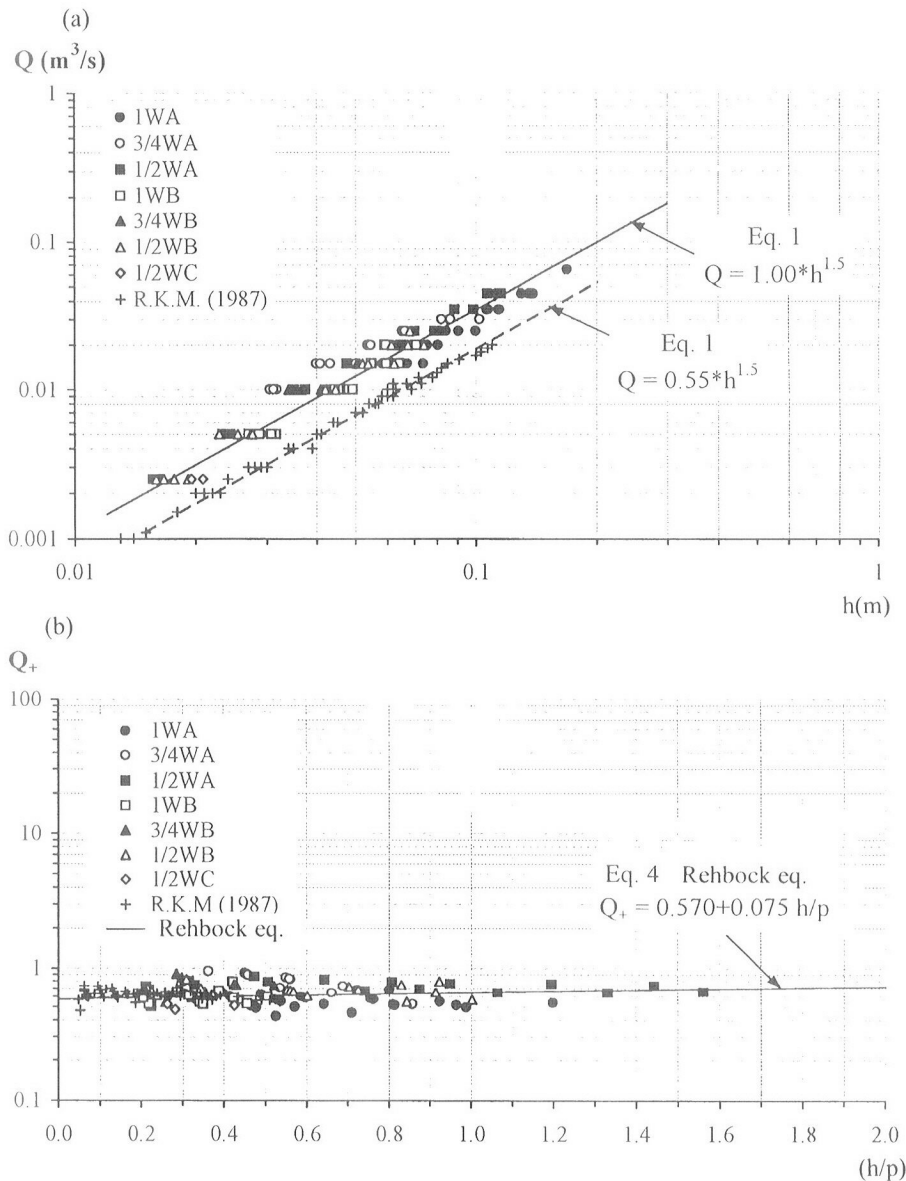
Figure 5c shows a transitional flow regime. The dominant flow features of this regime are the larger clockwise rotating cell, the elevated plunging jet, the absence of the surface eddy, and the wavy water surface. Figure 5d shows a transitional-baffle flow regime. This regime looks very similar to the plunging-transitional regime. However, the transitional-baffle regime occurs exclusively for the full weir height, A class weir spacing, and discharges greater than those required to maintain plunging-transitional flows. In this flow regime, the relatively smaller size of the weirs, compared to the size of the plunging jet, makes them act like baffles. Distinct features of this flow regime are the very wavy water surface and the location of the surface eddy closer to the downstream weir. A further increase in the flow rate makes the baffling action fully developed (see Fig. 5e) and the resulting flow regime is called baffle flow. In this flow regime, the line of impingement is located within the downstream half of the pool and moves further downstream as the discharge increases. Another distinct flow characteristic is the virtual disappearance of the surface roller.

Figure 5f shows a transitional-streaming flow regime that in part resembles the flow pattern of a fully developed stream-

ing flow shown in Fig. 5g. In a general sense, a transitional streaming flow regime has the clockwise circulating cell and the overriding surface flow similar to the streaming flow. However, influences from the transitional state still exist. Figure 5h shows the supercritical jet flow regime. It is simply a plunging jet that impinges on the bed to form a supercritical jet and is followed by a hydraulic jump.

The previous section addressed the different flow regimes that were observed for different arrangements of the weirs. The order in which these flow regimes were presented reflects the overall progression of the initial plunging flow regime passing through a transitional phase and into a final state of streaming flow. Two dimensionless parameters,  $Q_{t*}$  and  $L/p$ , were developed from these variables to predict the flow regimes. Figure 6 shows distinct domains for each flow regime and a number of interesting features. Firstly, plunging flows can occur for values of  $L/p$  greater than one, if the corresponding range of  $Q_{t*}$  is considered in the design. Secondly, although the typical value of  $L/p \approx 2$  has been used in most of the pool and weir fishways to achieve a plunging flow regime, this study reveals that a value of  $L/p \approx 3$  would be better in this regard. Thirdly, while only two flow regimes can form for values of  $L/p$  less than one, four flow regimes can form for values of  $L/p$  greater than four. Fourthly, the transition from plunging to streaming flow is a region, and is not described by a single value as suggested by Rajaratnam et al. (1988) from limited experimental observations. It should be noted that for a plunging flow to form, the value of  $L/p$  should be large enough for the plunging jet to impinge on the bed at or upstream of the base of the downstream weir. The study of Rand (1955) shows that for  $Q_{t*} = 0.01$ , the pool length has to be at least equal to the weir height for the plunging jet to impinge on the bed. Similarly, for the supercritical jet flow to occur, the pool length, in terms of the weir height, should be large enough for the jet to impinge on the bed and then to form a hydraulic

Fig. 7. Plunging flow (a) variation of  $Q$  with  $h$  and (b) variation of  $Q_+$  with  $h/p$ .



jump. Using the results of Bradley and Peterka (1957), it can be shown, with the consideration of the geometric and the flow conditions of this study, that the minimum length the jump takes to form on a sloping bed is about  $3p$ . This means that the minimum pool length required for the supercritical jet flow to form is about  $4p$ . The conditions of  $1/p \neq 4$  and  $4$  required for the formation of plunging flow and supercritical jet flow, respectively, are also referred to in Fig. 6.

**Flow equations for plunging and streaming flows**

Figure 7a shows the variation of  $Q$  with  $h$  on a log scale for plunging flows, using the experimental observations from this study and those of Rajaratnam et al. (1987). The lines drawn

through the data are not best fit lines but are plots of eq. [1] with the discharge coefficient  $C_d$  equal to 0.605 and  $b_0$  equal to 0.56 and 0.31 m, respectively. It should be noted that the data represented in Fig. 7a are for different weir heights, weir spacing, flume widths, and bed slopes. Hence, for the plunging flow,  $Q$  can be assumed proportional to  $h^{1.5}$ . Figure 7b shows the variation of  $Q_+$  versus  $h/p$  for the present data and those of Rajaratnam et al. (1987). Using Rehbock's equation (Kandaswamy and Rouse 1957) to estimate  $C_d$  in eq. [1] results in

$$[4] \quad Q_+ = \frac{Q}{b_0 \sqrt{g} h^{3/2}} = 0.570 + 0.075 \frac{h}{p}$$

Equation [4] fits the experimental data very well as shown in Fig. 7b. It shows that  $Q_+$  is a function of  $h/p$ . Rajaratnam et al. (1988) suggested a value of 0.61 for  $Q_+$ .

Fig. 8. Streaming flow (a) variation of  $Q$  with  $d$  and (b) variation of  $Q_*$  with  $L/d$ .

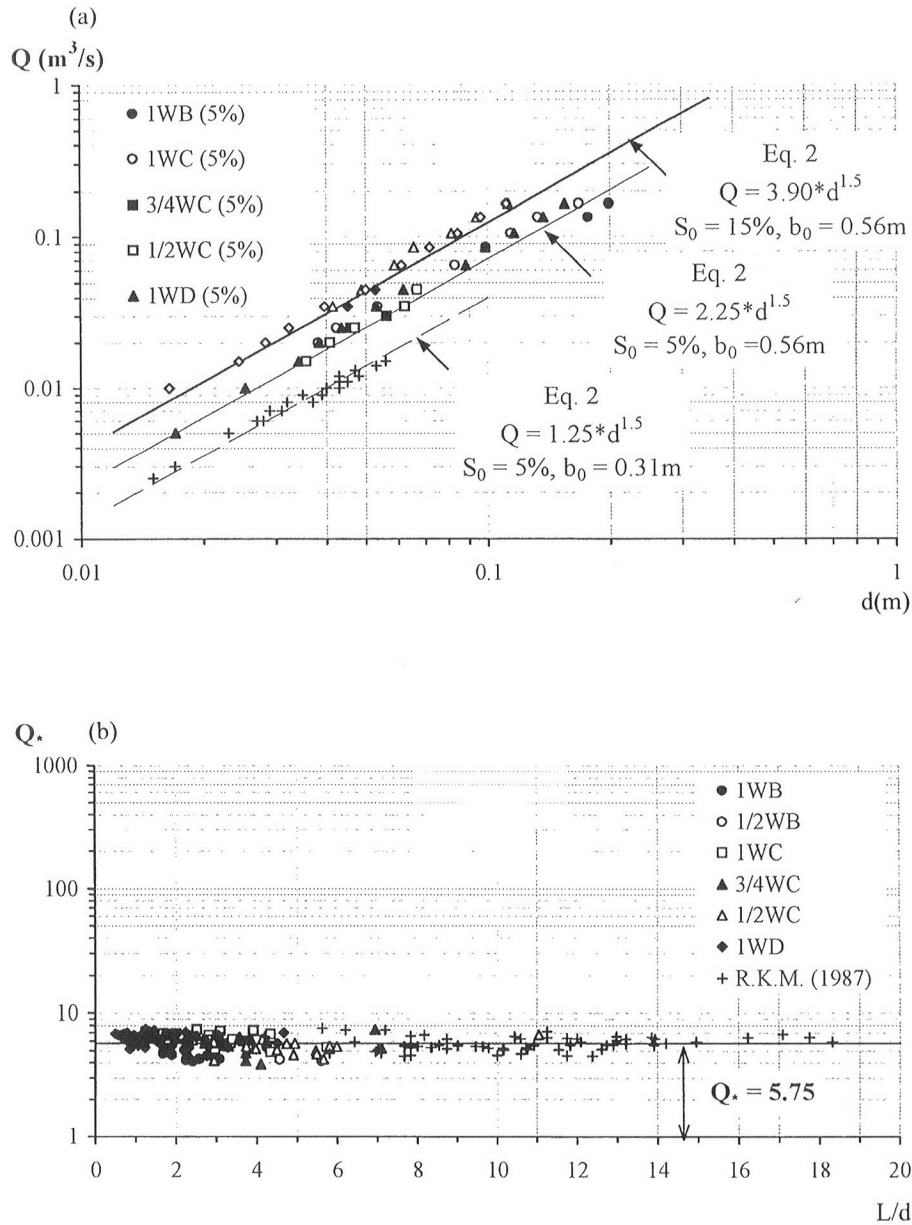


Figure 8a shows the streaming flow data, collected from this experimental study as well as those of Rajaratnam et al. (1987). Three groups of data were chosen for two different slopes (5% and 15%) and two different flume widths ( $b_0 = 0.31, 0.56$  m). Assuming a value of 0.06 for the coefficient of fluid friction  $C_f$ , eq. [2] was used to draw lines through the experimental data. Figure 8a shows that eq. [2] fits the experimental data reasonably well thereby suggesting that  $Q$  is proportional to  $d^{1.5}$ . Rajaratnam et al. (1988) stated that  $Q_*$  varies mainly with  $L/d$  from 3 to about 20. After a careful examination of the data of Rajaratnam et al. (1988), it was found that some experiments were conducted for relatively small streaming depths (less than

about 25 mm) where the scale effects due to surface tension might be present. Excluding these data and plotting the rest with the experimental results from this study in Fig. 8b,  $Q_*$  assumes a constant value of 5.75. Using this value in eq. [2] shows that  $C_f$  is a constant equal to 0.06.

**Velocity field and energy loss in pools**

The velocity profiles for plunging flows shown in Figs. 4a–4c are presented in Figs. 9a–9d. Figures 9a–9b show all the velocity profiles, located upstream and downstream of the impingement line, in a normalized form. In these figures,  $u$  is the

**Fig. 9.** Plunging flow (a) normalized velocity profiles in the pools, (b) variation of velocity scale, and (c) variation of length scale.

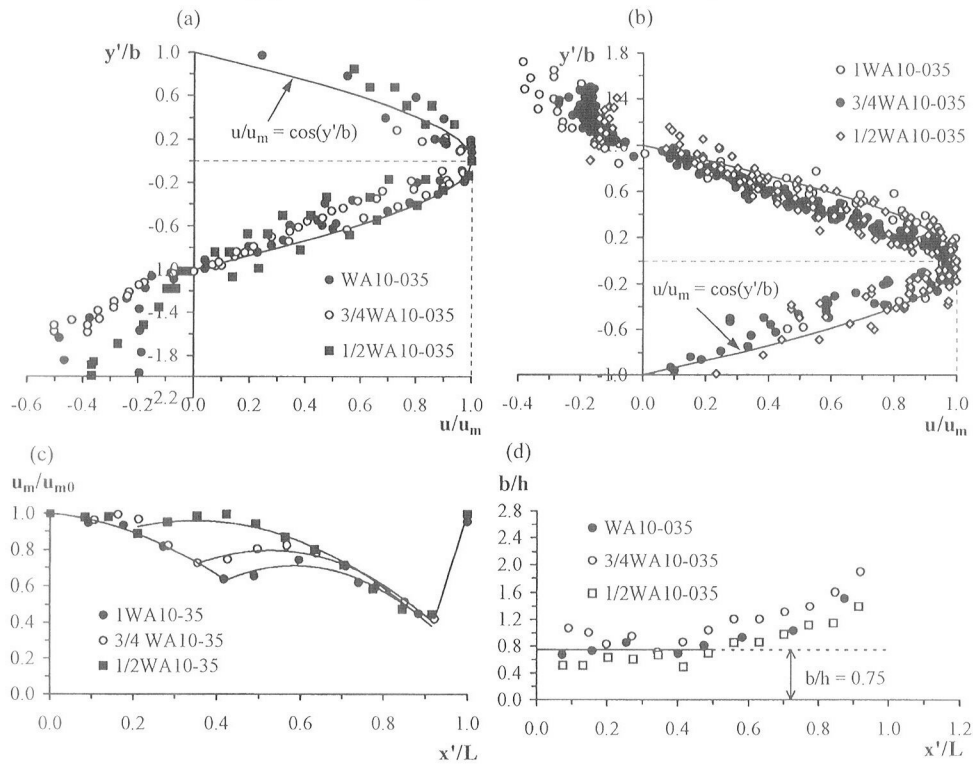
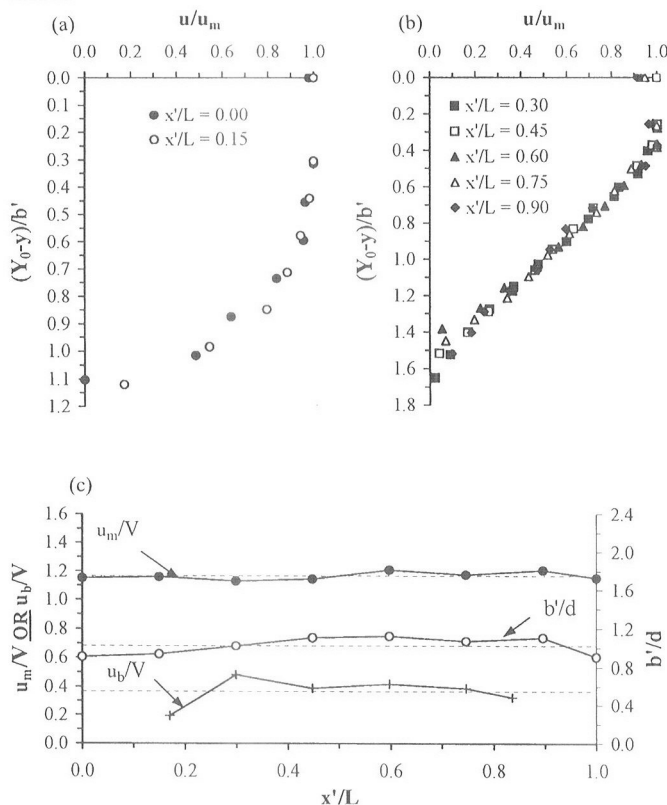


**Fig. 10.** Streaming flow (a) normalized velocity profiles in the developing flow region, (b) normalized velocity profiles in the develop flow region, and (c) variation of velocity and length scales.

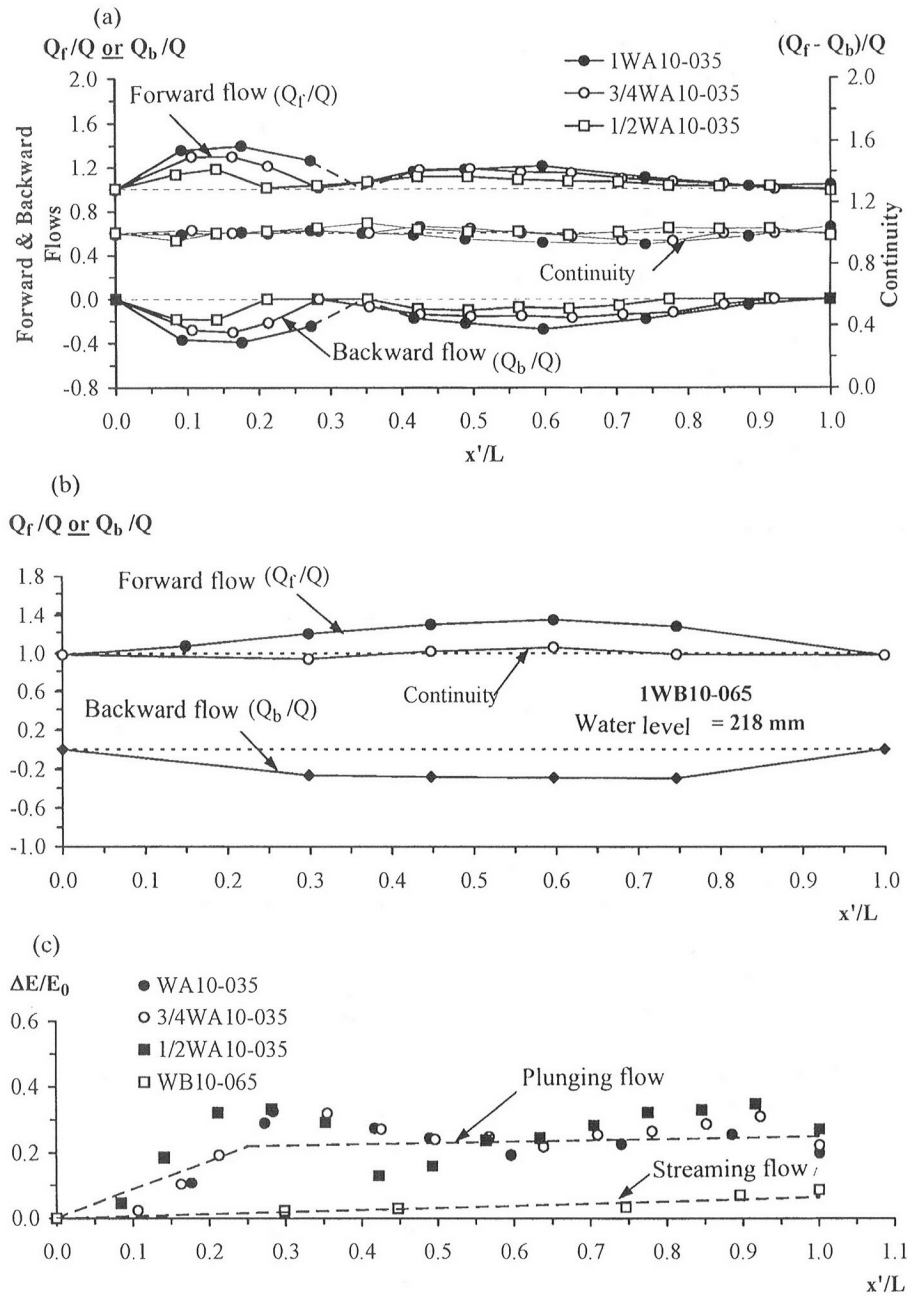


velocity component along the  $x$ -axis,  $u_m$  at any section is the maximum value of  $u$ ,  $y'$  is the perpendicular distance measured from the location of the maximum velocity, and  $b$  for any station is the vertical distance between the points of maximum velocity and zero velocity. Figures 9a–9b show that the forward velocity profiles, upstream and downstream of the impingement line, are similar and can be described approximately by a cosine-type equation

$$[5] \quad \frac{u}{u_m} = \cos \left\{ \frac{y'}{b} \right\}$$

Figures 9a–9b also show that the maximum return velocity near the bed within the confined eddy and in the surface eddy in terms of the maximum velocity at any station, is roughly equal to 0.5 and 0.4, respectively. Figures 9c–9d show the variation of the velocity and length scales with longitudinal distance  $x'$  measured along the  $x$ -axis from the crest of the upstream weir. The maximum velocity  $u_m$  is normalized with its value at the crest of the upstream weir,  $u_{m0}$ . Figure 9c shows that the maximum velocity  $u_m$  decays with distance until the jet impinges on the bed, after which it assumes a little recovery and then decays again until it reaches almost 40% of its original value at a distance of 90% of the pool length. Then, the maximum velocity assumes an abrupt increase until it regains its original value at the crest of the downstream weir. It was also found that  $u_{m0}/(2gh)^{0.5}$  is equal to 0.85 for the full height weir (which was slightly submerged) and 1.15 for the three quarters and the one half weirs. Figure 9d shows that the length scale  $b$ , normalized with the plunging head  $h$ , is equal to 0.75 up to the

Fig. 11. (a–b) Discharge variation and (c) energy dissipation in pools for plunging and streaming flows.



middle of the pool and then increases to about 1.50 near the downstream weir.

Velocity profiles for streaming flow shown in Fig. 4d were analyzed and the results are presented in Figs. 10a–10c wherein  $Y_0$  is the total depth of flow at any station,  $y$  is the perpendicular distance above the bed, and  $b'$  for any velocity profile is the distance measured from the water surface to the point where the velocity is  $0.5u_m$ . The first two velocity profiles, at  $x'/L = 0.00$  and 0.15, are plotted in Fig. 10a and the velocity profiles at other stations are plotted in Fig. 10b. From these figures, it appears that the velocity profiles are fully developed and are similar for  $x'/L$  greater than about 0.30. Figure 10c shows the variation of the velocity and length scales with longitudinal distance.

The maximum velocity  $u_m$  and the maximum return velocity near the bed  $u_b$  are normalized with the average velocity  $V$  equal to  $Q/b_0d$ , and the length scale  $b'$  is normalized with the streaming depth  $d$ . Figure 10c shows that  $u_m/V$ ,  $u_b/V$ , and  $b'/d$  are approximately constant and equal to 1.20, 0.36, and 1.00, respectively. It is interesting to see in Fig. 4d that the ceiling of the underlying eddy is almost the line connecting the weir crests which confirms that the discharge passing through the fishway is flowing with a constant layer of depth of  $d$ .

Figures 11a–11b show the discharge variation with distance for plunging and streaming flows, respectively. In these figures,  $Q_f$  and  $Q_b$  at any station, are the forward and backward discharges, respectively, and  $Q$  is the discharge in the fishway.

Figure 11a shows that the forward flow ratio  $Q_f/Q$  is equal to unity on the weir crests and at the intermediate line separating the two eddies (the confined eddy and the surface eddy). The discharge ratio has two peaks at the center of each eddy. The upstream peak is higher than the downstream one indicating that the confined eddy is more energetic than the surface eddy. The backward flow ratio  $Q_b/Q$  is equal to zero at the weir crests and has two minimum values corresponding to the forward flow peaks. The difference between the forward and the backward flows, normalized with  $Q$ , at any station along the pool is also shown in Fig. 11a where the result is very close to unity over the whole length of the pool, indicating the two dimensionality of the plunging flow in the pool and weir fishways. Taking into consideration the existence of only one cell of rotation in the streaming flow, similar observations on discharge variations along the pool can be found in Fig. 11b. Figure 11c shows the variation of the energy loss with the longitudinal distance for plunging as well as streaming flows. In this figure,  $\Delta E$  is the energy loss at any station and  $E_0$  is the total energy at the upstream weir. Figure 11c shows that, for plunging flows, almost 90% of the total energy loss occurs in the first quarter of the pool length confirming again the strength of the confined eddy. For the streaming flow, the energy loss increases linearly with the longitudinal distance.

## Conclusions

Based on the results of 435 experiments in a laboratory study of pool and weir fishways, over a wide range of slopes, length of pools, and height of weirs, the following conclusions are made. The flow regimes may be classified into plunging, transitional, streaming, and supercritical jet flows. It was found that the transitional regime encompasses several sub-regimes. A diagram has been developed to predict the different flow regimes using two dimensionless variables,  $Q_{t*}$  and  $L/p$ . This study also confirmed that discharge  $Q$  is proportional to  $h^{1.5}$  and  $d^{1.5}$  for plunging and streaming flows, respectively. The dimensionless discharge  $Q_f$  was found to follow the Rehbock equation while  $Q_b$  assumed a constant value of 5.75. The coefficient of fluid friction  $C_f$  is uniform over the pool length and equal to 0.06.

Velocity profiles in plunging as well as in streaming flows were found to be similar. Correlations have been developed for the velocity and length scales of these velocity distributions. The variation of the forward and backward flows with longitudinal distance has been evaluated. The variation of the energy loss with the longitudinal distance in the pool was studied and it was found that in plunging flows, almost 90% of the total energy loss occurs in the first 25% of the pool. In the streaming flow, the rate of the energy dissipation was found to be uniform

over the length of the pool. If the present work is considered to be a scale model study, the scale of these models will be approximately 10.

## Acknowledgments

This research work was performed at the T. Blench Hydraulics Laboratory of the University of Alberta, Edmonton, Canada, with the financial support of Fisheries and Oceans Canada and the Natural Sciences and Engineering Research Council of Canada. The authors are thankful to S. Lovell for building the experimental arrangement.

## References

- Bradley, J.N., and Peterka, A.J. 1957. Hydraulic design of stilling basins: Stilling basin with sloping apron (Basin V). *J. Hydraul. Div., Am. Soc. Civ. Eng.* **83**(HY5): 1-32.
- Clay, C.H. 1961. Design of fishways and other fish facilities. Department of Fisheries of Canada, Ottawa, Ont.
- Kandaswamy, P.K., and Rouse, H. 1957. Characteristics of flow over terminal weirs and sills. *J. Hydraul. Div., Am. Soc. Civ. Eng.* **83**(HY4): 1-13.
- Katopodis, C. 1995a. On developing sturgeon fishways. Technology Research Center for Riverfront Development. *In Proc. Sapporo Session on Fish Passage for Northern Countries*, Sapporo, Japan, 20 October 1995, pp. 35-53.
- Katopodis, C. 1995b. Recent fishway design problems in Canadian rivers. *In Proc. International Symposium on Fishways 95*, Gifu, Japan, 24-26 October 1995, pp. 1-7.
- Katopodis, C. 1999. Sustaining fish migrations: swimming performance and fish passage/exclusion methods. *In Proc. Nordisk Symposium om Fiskepassasjer / Nordic Conference on Fish Passage*, Oslo, Norway, 9-11 September 1998, pp. 23-30.
- Rajaratnam, N., and Muralidar, D. 1967. Yaw and pitch probes. Hydraulic Instrumentation Series, Department of Civil Engineering, University of Alberta, Edmonton, Alta.
- Rajaratnam, N., Katopodis, C., and Mainali, A. 1987. Pool and weir fishways. Report WRE 87-1, Department of Civil Engineering, University of Alberta, Edmonton, Alta.
- Rajaratnam, N., Katopodis, C., and Mainali, A. 1988. Plunging and streaming flows in pool and weir fishways. *J. Hydraul. Eng., Am. Soc. Civ. Eng.* **114**(8): 939-944.
- Rand, W. 1955. Flow geometry at straight drop fishways. *J. Hydraul. Div., Am. Soc. Civ. Eng.* **81**(HY9): 1-13.
- Sikora, G.J. 1997. An experimental study of flow regimes in pool and weir fishways. M.Sc. thesis, Department of Civil Engineering, University of Alberta, Edmonton, Alta.
- Sikora, G.J., Rajaratnam, N., and Katopodis, C. 1996. A photographic study of pool and weir fishways. Tech. Report-SRK1, Department of Civil Engineering, University of Alberta, Edmonton, Alta.